Analysis of the Gas Flow in a Labyrinth Seal of Variable Pitch

D. Joachimiak[†] and P. Krzyślak

Chair of Thermal Engineering, Poznan University of Technology, Poznań, 60-965 Poznań, Poland

†*Corresponding Author Email: damian.joachimiak@put.poznan.pl*

ABSTRACT

The paper discusses the results of investigations performed for the segments of straight-through labyrinth seals of constant length. Increasing the number of teeth of a segment resulted in a reduction of the pitch length to obtain the slot seals. The phenomena occurring during gas flow in labyrinth and slot seals differ significantly. They are described with different calculation models. The analysis presented in this paper is related to the change of the tightness and the nature of the flow from a straight-through labyrinth seal to a slot seal. The paper includes the results of experimental research and CFD calculations. Models applied for the Neumann and Scharer labyrinth seals as well as the model of the Salzman and Fravi slot seals were discussed. For the Neumann and Scharer models, correction coefficients for the tested geometry were proposed. Based on the assumptions for the said models and the obtained results, the phenomena responsible for the minimization of the leakage were discussed. The leakage rate in segments of different gap heights depending on the number of teeth and the pressure ratio upstream and downstream of the segment has been analyzed. Based on the experimental data, an optimum number of teeth in the segment for minimum leakage was determined. CFD calculations allowed determining the minimum leakage geometry. The experimental data contained in this paper confirm that the determined optimum pitch range is independent of the pressure drop.

Keywords: Slot seal; Flow machines; Leakage; CFD; Optimization.

NOMENCLATURE

A	clearance flow area	σ	mass flow correction parameter (in the Salzman and Fravi method)
B	teeth thickness		
C_f	coefficient of flow	λ	coefficient of linear losses
D	diameter of the seal	μ	coefficient of kinetic energy carry-over
f	function	η	dynamic viscosity
H	height of the seal segment	β	parameter included in the coefficient of flow
HG	height of the gap		
K	constant (in the Salzman and Fravi method)	δ	relative error
		γ	correction parameter
LS	length of the segment		
L	pitch	Subscripts	
$\dot{m}$	mass flow	c	critical parameter
p	absolute pressure	01	total parameter upstream of the segment
R	specific gas constant	2	static parameter downstream of the segment
Re	Reynolds number		
t	number of teeth	SF	Salzman and Fravi
T	temperature	S	Scharrer
u	axial velocity	max	maximum value
y	dimension in the radial direction	min	minimum value
y'	dimensionless gap height	N	Neumann
		i	i-th tooth
α	parameter included in the coefficient of kinetic energy carry-over	e	experiment
		e-4t	a data from the experiment for the reference geometry (t=4)
κ	ratio of specific heats		
v	specific volume	F	Fluent

s   static parameter

e, e-4t   value from the experiment compared with the results of the experiment for the reference geometry

F, e-4t   value from the Fluent software compared with the results of the experiment for the reference geometry

1. INTRODUCTION

Labyrinth seals are widely applied in a variety of flow machines. Their task is to minimize the leakage. Straight-through labyrinth seals are applied in steam turbines, in spots far from the thrust bearings (Trütnovsky, 1964). Such seals are fitted both as turbine external seals and shroud seals.

Straight-through labyrinth seals of small chambers size are also applied in piston cylinder pairs of combustion engines (Larjola *et al.,* 2010). An additional aspect of the seals applied in combustion engines is their impact on the exhaust emissions. Labyrinth seals are highly impactful on the efficiency of the said machines. The optimization of the geometry of labyrinth seals aims at minimizing the leakage. This leads to greater efficiency of the machines and increases safety of operation. The first calculation model describing the flow of gas in a straight-through seal was developed by Martin (1908). Egli (1935) and other researchers such as Hodkinson (1940), Zimmermann and Wolff (1987) included the kinetic energy carry-over and the influence of the contraction of flow in their calculation models. These models were further developed by Neumann (Childs and Scharrer, 1986) and Scharrer (1988) who proposed a method of calculating of the tooth-by-tooth leakage in the seal. The carry-over effect of the kinetic energy depends on the geometry of the seal (pitch, chamber size) and is significantly influenced by the degree of wear and tear of the seal (Joachimiak and Krzyślak, 2017).

The results of the experimental research and the CFD calculations of the flow in a straight-through labyrinth seal are included in Yuan *et al.* (2015). The CFD calculations were carried out within the framework of OpenFOAM. In this paper, the influence of the lengths and depths of the chamber on the extent of the leakage was investigated. In Anker *et al.* (2002), a numerical analysis of the flow in a two-tooth over-shroud straight-through labyrinth seal in a stage of a low speed axial turbine was presented; the authors analysed the impact of the leakage on the main flow. This paper proved a significant impact of the leakage on mixing losses and secondary flows that generate considerable energy loss in the stage of the turbine. In Schramm *et al.* (2004), a numerical method of optimization of the shape of the stepped labyrinth seal was presented. Stępień and Kossowski (2009) as well as Stępień *et al.* (2003) include the analysis of the flow in a straight-through over-shroud seal in a turbine stage. The presented investigations were related to the geometry of the straight-through labyrinth seal of different configuration and number of sealing teeth. Zhang *et al.* (2014) made CFD calculations of the over-shroud seal of an axial turbine. The calculations were performed for the geometry of a two-tooth straight-through labyrinth seal. The results of the

calculations were compared with the proposed geometry of the seal on the sidewalls of the shroud. In Lampart (2007), the influence of the shroud leakage on the operating parameters of the axial turbine stage was analyzed.

The concept of the free piston engine was presented in Larjola *et al.* (2010). Between the piston and the cylinder, a straight-through labyrinth seal was applied. This solution enabled oil free operation. In order to determine the leakage of compressible and non-compressible media in straight-through labyrinth seals, a modified Stodola method was used (Martin, 1908). In the presented model, an isothermal flow was assumed. This method was adapted for the calculations of groove seals. The analysis of the influence of the pitch length, chamber size or tooth thickness on the level of leakage was included in Trütnovsky (1964).

In Nayak *et al.* (2016), the coefficients of flow in a straight through labyrinth seal of a smooth surface and honeycomb type surface have been compared. The theoretical mass flow was determined with the modified Zimmermann and Wolff method. The analysis was performed for two different slot heights, chamber sizes and pressure ratios. Numerical research of the gas flow in the honeycomb seal has also been presented by Frączek *et al.* (2017). The paper presents the influence of the change in geometry parameters such as position and height of the teeth on the reduction of the leakage.

For high degree of wear and tear of the straight-through labyrinth seal, the gas flow is accompanied by a fading expansion effect in the slots. As a result, the nature of the gas flow becomes similar to that of the slot seal (Joachimiak and Krzyślak, 2017). A drop in the pressure in the slot seals does not result from the expansion of the working medium as much as it is in the case of straight-through labyrinth seals. The drop in the pressure in the slot seals is mainly caused by the velocity-reducing shear stresses between the fluid and the walls. For this reason, the nature of the gas flow in the slot seals (Trütnovsky, 1964) differs from that of the labyrinth seals and is described with different assumptions. The calculation model describing the gas flow allowing for friction in the slot seal has been included in Joachimiak and Krzyślak (2016). The presented model is based on the balance of total enthalpy. It includes dissipation of gas kinetic energy into heat and the friction between the gas and the seal walls, presented by a modified coefficient of friction based on the Blasius equation. Yamada (1962) has presented a pressure loss for water flow in slotted groove seals with a coefficient of linear losses. In Mel'nik (2009), a method of the calculation of leakage of an incompressible fluid in short slot seals has been described. This method is based on experimentally determined relations between the coefficient of local losses and the linear coefficient

of pressure loss. Asok (2007) describes characteristics of the pressure drops and the water leakage in a straight-through labyrinth seal. The analysis pertained to the influence of the geometry of the chambers of straight and curved (optimized) walls on the extent of leakage. A semi-theoretical model enabling the determination of the pressure drop was presented. Two new coefficients determining the velocity in the chambers and the swirl losses were proposed. The calculations were performed for different chamber geometries.

At the stage of designing a flow machine, the spot where the seal is to be located is usually determined with dimensions. For the set length and nominal size of the gap of the straight-through labyrinth seal, a geometry characterized with a minimum leakage is vital. The paper presents the problem of the influence of the number of teeth (hence the length of the pitch) on the extent of the leakage at a segment length of 31 mm. It also includes the analysis of the change of the leakage and the nature of the flow from a straight-through labyrinth seal to a slot seal. The analyzed geometry of seals is applied, inter alia, in steam turbines, pumps, compressors and gas turbines. Therefore, the research problem has a wide technical application.

2. SCOPE OF EXPERIMENTAL RESEARCH

Test stand used for the research (Fig. 1) included a compressor, a compressed air tank, a mass flow measuring system, a model segment of the seal and the measurement system.
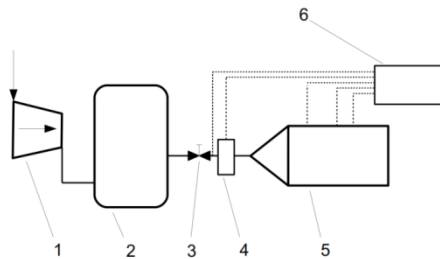

Fig. 1. Test stand: Diagram of the test stand for testing labyrinth seals, 1 - compressor, 2 - main tank, 3 - regulator valve, 4 - orifice, 5 - body, 6 – measurement system.

In the body (Fig. 1.), there was an internal part (insert) (Figs. 2, 3), on which the seal model was fitted. In the experimental research, absolute pressure transmitters of the measurement range of 0-$5 \cdot 10^5$ Pa and the measurement accuracy of $\pm 0.25\%$ and pressure difference transmitters of the measurement range of 0-$0.25 \cdot 10^5$ Pa and the measurement accuracy of $\pm 0.2\%$ were used. For the measurement of the temperature, T thermocouples were applied. The measurement of the mass flow was performed with an orifice with a near-disc pressure measurement. The measurement system of the test stand allowed measuring the mass flow passing through the segment, the static pressure and the temperature upstream and downstream of the segment as well as the temperature of the body.
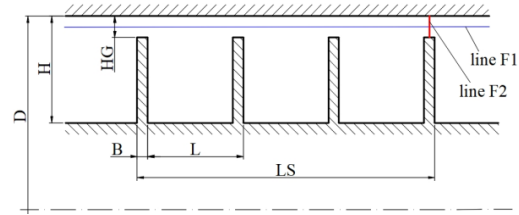

Fig. 2. Geometry of the model segment of the seal.

Table 1 Geometry dimensions

Mark	Name	Size [mm]
D	Diameter of the seal	150
LS	Length of the segment	31
H	Height of the seal segment	10
HG	Height of the gap	0.362 0.542 0.752
B	Tooth thickness	1
L	Length of the pitch	(Table 2)

Fig. 3. Internal part (insert) with 11 teeth.

The experimental research concerns the segment of the straight-through seal of the height of HG 0.362, 0.542, 0.752 mm, constant segment length of LS 31 mm and tooth thickness B of 1 mm (Table 1). The experimental research was performed for the segments containing 4, 6, 11 and 31 teeth. The geometry of the seal containing 31 teeth, in which the pitch equals the thickness of the tooth L=B=1 mm represents a slot seal. The lengths of the pitch for the analyzed segments have been shown in Table 2.

Table 2 Variants of the segment geometry of a constant length of 31 mm included in the experimental and CFD research

Number of teeth - t	Pitch – L [mm]
4	10
6	6
9	3.75
11	3
12	2.727
13	2.5
17	1.875
21	1.5
24	1.304
31	1 (L = B)

The main information related to the nature of the gas flow in the segment of the seal obtained from the experimental data for the analyzed geometries is the mass flow for the determined total pressure upstream and static pressure downstream of the segment. The experimental data and CFD calculations contained in the paper led to the selection of such a pitch for the straight-through seal that resulted in minimum leakage. The results obtained in the research work will allow investigating the change of the gas flow specificity in the discussed seal geometries.

3. ONE DIMENSIONAL CALCULATION METHODS

The flow of gas in the seals results from the pressure gradient. The mass flow passing through the slot seal is limited with shear stresses between the gas and the seal wall. The Salzman and Fravi method (Trütnovsky, 1964) was applied to determine the mass flow of gas passing through the slot seal. The reference value is the mass flow resulting from the critical flow described with a formula

$$\dot{m}_c = A \left(2 \frac{\kappa}{\kappa+1} \frac{p_{01}}{v_{01}} \right)^{0.5} \left(\frac{2}{\kappa+1} \right)^{\frac{1}{\kappa-1}} \tag{1}$$

The actual mass flow is determined by the relation (Trütnovsky, 1964)

$$\dot{m}_{SF} = \sigma \dot{m}_c \tag{2}$$

Parameter σ depends on the type of gas determined with the isentropic exponent κ, on the—Reynolds number, on the friction factor in the seal λ, the ratio of the pressure upstream of the segment to the pressure downstream of the segment and the seal geometry (Trütnovsky, 1964):

$$\sigma = f \left(\kappa, \mathrm{Re}^*, \lambda, \frac{p_{01}}{p_2}, LS, HG \right) \tag{3}$$

In this method the Reynolds number is defined as

$$\mathrm{Re}^* = K \frac{HG \sqrt{p_{01}/v_{01}}}{\eta} \tag{4}$$

where K is a constant depending on the type of gas.

The mass flow of gas in the labyrinth seal is reduced by the conversion of the energy of pressure to the kinetic energy in the slots and dissipation of kinetic energy in the seal chambers into heat. One of the semi-empirical methods allowing the determination of the mass flow of the gas passing through a labyrinth seal is the Neumann equation (Childs and Scharrer, 1986)

$$\dot{m}_{Ni} = C_{fi} \mu A \sqrt{\frac{p_i^2 - p_{i+1}^2}{RT}} \tag{5}$$

This method consists in tooth-by-tooth analysis of the gas flow in the seal. It contains a semi-empirical coefficient of flow that allows for the contraction of flow downstream of the gap

$$C_{fi} = \frac{\pi}{\pi + 2 - 5\beta_i + 2\beta_i^2} \tag{6}$$

where $\beta_i = \left(\dfrac{p_i}{p_{i+1}} \right)^{\frac{\kappa-1}{\kappa}} - 1$.

Equation (5) contains the coefficient of kinetic energy carry-over μ defined as

$$\mu = \left(\frac{n}{n(1-\alpha_{Ni}) + \alpha_{Ni}} \right)^{0.5} \tag{7}$$

where $\alpha_{Ni} = 1 - (1 + 16.6 HG/L)^{-2}$.

Another method of determining the mass flow in a straight-through labyrinth seal included in the analysis is the Scharrer method (Scharrer, 1988) that additionally allows for the thickness of the tooth B_i. This method is based on the Neumann Eq. (5) and the coefficient of flow C_{fi} formulated with Eq. (6). Scharrer (Scharrer, 1988) defined the coefficient of kinetic energy carry-over with the following formula

$$\mu = \left(\frac{1}{(1-\alpha_{Si})} \right)^{0.5} \tag{8}$$

where $\alpha_{Si} = \dfrac{8.52}{(L-B)/HG + 7.23}$.

4. SCOPE OF CFD CALCULATIONS

The CFD calculations were performed in Fluent 13.0 environment. The geometry has an inlet portion of the length of 2LS. Behind the last tooth, a swirling gas is expected, which is why the length of the outlet portion was assumed at 3.5LS. The geometry of the calculation domain has been shown in Fig. 4.

Fig. 4. Calculation domain.

A calculation 2D mesh was created for axisymmetric geometry. For the geometry of 4 teeth, the mesh is composed of approx. 271500 elements and 274500 nodes. In the wall layers, 20 grid cells of the mesh were assumed. In the calculations, a k-ω SST (shear stress transport) turbulence model was applied. In order to meet the mesh quality requirements for the SST k-ω model in the wall layer, a condition $y^+ < 2$ was applied. The mesh for L=10 mm has been shown in Fig. 5.
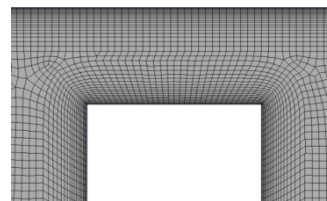

Fig. 5. Mesh used for the calculations around the gap of the geometry of HG = 0.542 mm.

Based on the experimental data, in the inlet plane, total pressure was assumed while in the outlet plane static pressure was assumed. In the CFD calculations the temperature of the gas, the body and the insert were assumed based on the experimental data. In this paper, stationary 2D RANS calculations were presented. The equations of conservation of mass, momentum and energy were also included. The calculations were performed for the air treated as an ideal gas. The stationary calculations were performed using the Pressure Based Coupled Solver (PBCS). In the calculations Convergence Tolerance of 10^{-6} was assumed. A k-ω SST turbulence model was applied (Menter, 1994). It is used since it combines merits of models k-ε and k-ω. Model k-ω SST uses the k-ω model in the boundary layers where it model well the turbulent flow and has a significant influence on the nature of flow in the regions of seal gaps. It changes automatically into k-ε in regions of free-stream flow and in the shear layers. Moreover, it has an element limiting the overproduction of turbulence kinetic energy in stagnation regions and regions with strong acceleration.

5. RESULTS

Table 3 presents the experimental data obtained for 4 different pitches of the straight-through seal: 10, 6, 3 and 1 mm (slot seal). The CFD calculations were carried out for a greater number of seal geometries. This allowed an obtainment of more accurate data related to the change of the nature of the flow between the straight-through and the slot seals. In this part, the experimental and CFD data shown in Table 3, were obtained for the ratio of the total pressure upstream of the segment to the static pressure downstream of the segment $p_{01}/p_2 = 2$.

Table 3 Results of the experimental research and CFD calculations for HF = 0.542 mm and $p_{01}/p_2 = 2$

Number of teeth t	$\dot{m}_e$ [kg/s]	$\dot{m}_F$ [kg/s]	$\delta\dot{m}_{F,e}$ [%]	$\delta\dot{m}_{e,e-4t}$ [%]	$\delta\dot{m}_{F,e-4t}$ [%]
4	0.0743	0.0745	-0.3	0	0.25
6	0.0719	0.0724	-0.7	3.2	-2.6
8	–	0.0717	–	–	-3.5
9	–	0.0716	–	–	-3.6
11	0.0720	0.0723	-0.4	3.1	-2.8
12	–	0.0728	–	–	-2
13	–	0.0733	–	–	-0.7
17	–	0.0743	–	–	2
21	–	0.0760	–	–	3.9
24	–	0.0809	–	–	8.8
31	0.0873	0.0857	1.82	-17.5	15.3

For the analyzed geometries (Tables 1, 2) and the measurement data (Table 3), the mass flow was calculated for the labyrinth segment of a slot seal with the Neumann, Scharrer as well as Salzman and Fravi methods.

Assuming the geometry of 4 teeth (t=4) as the reference geometry, the correction coefficients γ, being constants for other geometries under

consideration, were determined respectively. For the Neumann method

$$\dot{m}_{Ni} = \gamma_N C_{fi} \mu_{Ni} A \sqrt{\frac{p_i^2 - p_{i+1}^2}{RT}} \quad , \quad \text{where}$$

$$\gamma_N = \frac{\dot{m}_e}{\dot{m}_{Ni}} \quad (9)$$

and for the Scharerr method

$$\dot{m}_{Si} = \gamma_S C_{fi} \mu_{Si} A \sqrt{\frac{p_i^2 - p_{i+1}^2}{RT}} \quad , \quad \text{where}$$

$$\gamma_S = \frac{\dot{m}_e}{\dot{m}_{Si}} \quad (10)$$

For the reference geometry (t = 4), $\gamma_N = 1.16$, $\gamma_S = 1.37$ were obtained.

Figure 6 presents values of mass flow for the analyzed segments (Fig. 2, Tables 1, 2, 3) with a number of teeth ranging from 4 to 31, obtained in the experiment, from the Fluent software and calculated usig the corrected Neumann's and Scharrer's methods for the labirynth seals and the Salzman-Fravi method for the slot seal.
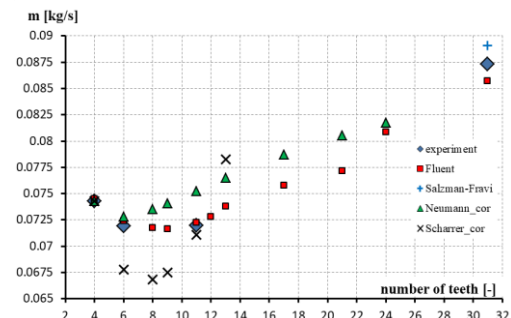

Fig. 6. Mass flow obtained in the experiment, by Fluent, and with the use of the corrected Neumann and Scharerr methods for the labyrinth seal and Salzman-Fravi method for the slot seal.

It results from Fig. 6 that the curve of variability of the mass flow is well reproduced by the corrected Neumann method. One can see a minimum for six teeth where the mass flow obtained with this method is close to the value obtained in the experiment. The mass flow obtained with the Scharer method differs from the experimental data for the segment with 6, 8, 9 and 11 teeth. Yet, this method determines more accurately the number of teeth for the minimum of the mass flow. For the slotted segment, a good accuracy of the mass flow obtained with the Salzman and Fravi method was observed.

The maximum relative error of the mass flow between the experimental data and the data obtained in the Fluent software is 1.82% (Table 3). This is a result for the slotted segment. The minimum error was obtained for the segment containing 4 teeth. Its value was -0.3%.

For the segment of 4, 6 and 11 teeth, a good convergence of the CFD calculations with the

experimental data was observed. It results from the experimental data that the smallest mass of air flows through the segments with the number of 6 to 11 teeth, achieving the values of 0.0724 and 0.0723 kg/s, respectively. This relation is confirmed by the CFD calculations. From the data presented in Fig. 6, it also results that in the segments of the number of teeth ranging from 13 to 31, the mass flow grows significantly from 0.0733 to 0.0857 kg/s. Assuming that the segment containing 4 teeth is a reference geometry, a relative change in the mass flow was determined in the experiment for the outstanding, experimentally analyzed segments.

$$\delta \dot{m}_{e,e-4t} = \frac{\dot{m}_{e-4t} - \dot{m}_e}{\dot{m}_{e-4t}} \cdot 100\% \qquad (11)$$

A relative change in the mass flow obtained in the Fluent software referred to the mass flow obtained in the experiment for the reference geometry containing 4 teeth was defined as

$$\delta \dot{m}_{F,e-4t} = \frac{\dot{m}_{e-4t} - \dot{m}_F}{\dot{m}_{e-4t}} \cdot 100\% \qquad (12)$$

Figure 7 presents the percentage change of the mass flow obtained in the measurements and in the Fluent software. These results are referred to the mass flow obtained in the experiment for the 4-tooth segment.
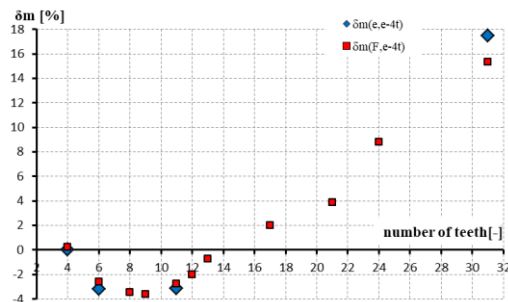

Fig. 7. Relative change in the mass flow obtained in the experiment δm$_{e,e-4t}$ and in the Fluent δm$_{F,e-4t}$.

The spread of the relative change of the mass flow for the analyzed geometries reaches almost 19% (Fig. 7). A relative decrease in the leakage defined according to Eq. (12) for the segments containing 6 and 11 teeth is almost equal and amounts to 3.2 and 3.1%, respectively. The lowest mass flow of the value of 0.0716 kg/s (Fig. 7) was obtained for the segment containing 9 teeth. It was lower by 3.6% than the value obtained for the reference geometry.

In order to explain the influence of the number of teeth in the segment of constant length on the level of leakage, an analysis of the fields of velocity in selected geometries was performed. The leakage of the segment of the seal is influenced by the phenomena occurring during the flow of gas. In the gaps, the gas increases its velocity and decompresses at the same time (Fig. 8). The gas flow at the outlet of the seal chamber has a high velocity. This velocity is reduced in the chamber as a result of kinetic energy dissipation in the form of heat.

In segment 4t ((L-B)/H=0.9) high gas velocity of the maximum value of approx. 80 m/s occurs in the entire volume of the chambers (Fig. 8(a)). Immediately, downstream of the gaps and in the chamber corners, small swirls are visible of the velocity of approx. 25 m/s. Segment 6t (Fig. 8(b)) is characterized by the ratio of the chamber sides (L-B)/H= 0.5. In this segment, in each of the chambers, two gas swirls occur of the velocities of 90 and 40 m/s. For this geometry, the gas velocity in each of the five chambers between the gaps decreases heavily (Figs. 8(b), (9)). Segment 9t ((L-B)/H= 0.28) is characterized by at least three swirls occurring in the chambers of the velocities close to the values of 75, 50 and 25 m/s (Fig. 8(c)). In segments 9t and 11t a significant swirl velocity of the gas (approx. 60 m/s) occurs in an increasingly smaller volume of the chambers (Figs. 8(c), (d)). In the outstanding volume, the gas swirl velocity is fading. Despite the differences in the geometries and the velocity fields, segments 6t and 11t are characterized by a similar mass flow (Figs. 6, 7).
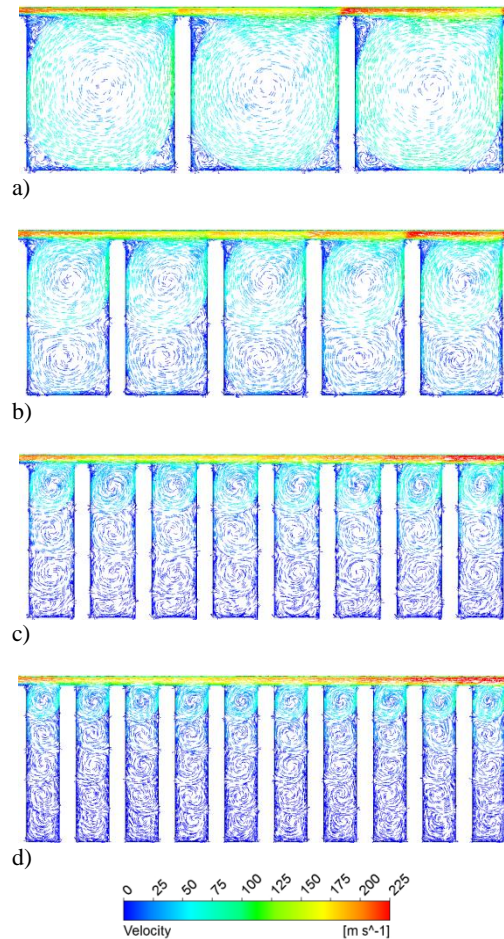

Fig. 8. Vectors of the fields of velocity in the segments having: a) 4, b) 6, c) 9 and d) 11 teeth and the ratios of the sides of the chamber (L-B)/H of : 0.9, 0.5, 0.28 and 0.2.

In order to present the differences characterizing the flow of gas in the analyzed segments more clearly, axial velocities of the gas, obtained in the Fluent software, read from the F1 line located at half of the

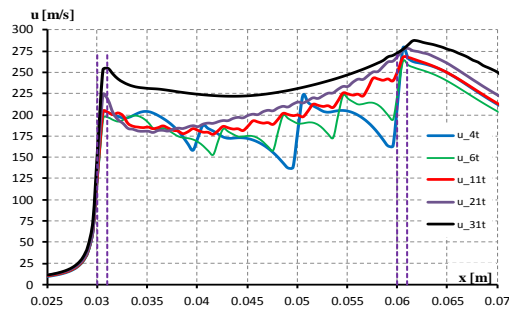gap height (Fig. 2), were presented.

Fig. 9. Velocity distribution in the axial direction in the seal of the number of teeth 4 - 31 for HG = 0.542 mm, obtained in the Fluent (line F1, Fig. 2.). The dashed lines denote the walls of the first and the last tooth.

For all geometries, the greatest acceleration of gas occurs in the inlet area in the initial section of the seal and it depends on the value of the leakage (Table 3). For the analyzed geometries, the velocity of gas at the outlet from the segment has similar values. For the segments containing 4 and 6 teeth, the velocity of gas clearly increases in the area of the gaps. For these geometries we can also observe a reduction of the velocity in the chamber between the gaps (Figs. 8(a), (b)). The higher the number of teeth, the lower the acceleration of the gas in the gaps and the drop of velocity in the chambers. Hence, an increase in the number of teeth in the seal changes the gas axial velocity that approximates that of a gap seal. A relatively small change in gas velocity as a result of the constant flow field is observed along the slot seal length.

Figure 9 presents the change of the static pressure in selected segments of the seal. The data were read from the F1 line (Fig. 2).
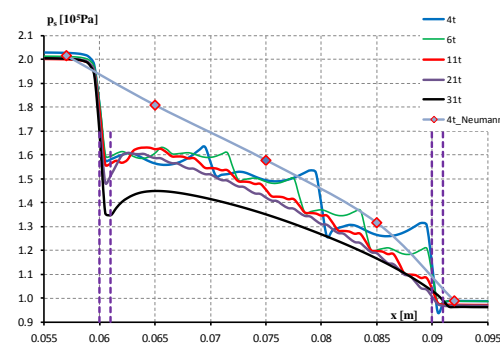

Fig. 10. Distribution of static pressure in the seal (t from 4 to 31) obtained in Fluent (line F1, Fig. 2) and the pressure inside the chambers of the 4-tooth segment obtained with the Neumann method.

In the analyzed geometries, a significant decompression of gas occurs in the area of the first gap (Fig. 10). For the seal containing 4 teeth, the pressure drop is the lowest and amounts to $0.5 \cdot 10^5$ Pa, while for the slot seal, it is the highest and amounts to $0.65 \cdot 10^5$ Pa. In a segment containing 4

teeth, the pressure drop increases starting from the second gap. The greater the number of teeth in the segment, the lower the drop of static pressure in the gaps. A change in the static pressure in a slot seal has a similar course to heavily worn straight-through 4 tooth seals (gap height HG = 1.5 and 2 mm) presented in Joachimiak and Krzyślak (2017). The data in Figs. (8), (9) and (10) present the transition of the nature of the flow from that characteristic of the labyrinth seal to the one characteristic of the slot seal.

The gas flowing through a segment of the seal is gradually decompressed. The highest gas velocities occur in the last gap of the segment, where the lowest static pressure occurs (Fig. 10). Figure 11 presents the distributions of velocities in the last gap of the seal obtained in the Fluent software . The gap height was described with a dimensionless parameter

$$y' = \frac{y - y_{min}}{y_{max} - y_{min}} \quad (13)$$

where y_{min}, y_{max} − extreme dimensions of the gap in the radial direction.

The distributions of the axial velocity were read from the F2 line located at half of last tooth thickness (Fig. 2) for segments 4t, 6t, 9t and 11t (Fig. 11). The average values for the analyzed velocities of the equation were calculated according to the formula

$$u_{av} = \frac{1}{HG} \int_{y_{min}}^{y_{max}} u(y) dy \quad (14)$$

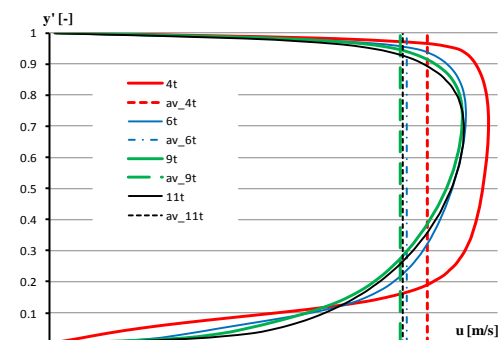where $HG = y_{max} - y_{min}$.

Fig. 11. Distribution of the gas axial velocity in the last gap of the seal and the average values (vertical lines) for segments 4t, 6t, 9t and 11t ($p_{01}/p_2 = 2$).

The greatest velocity field of the maximum value of 284 m/s and the average value of 244 m/s was obtained for segment 4t (Fig. 11). For segments 6t, 9t and 11t, the velocity profiles have similar courses with the maximum value of approx. 268 m/s. The lowest average was obtained for segment 9t of the value of 226 m/s. Axial velocity distributions confirm the relations among the values of the mass flow obtained for the segments under analysis.

6. ANALYSIS OF THE LEAKAGE OF SEGMENTS OF DIFFERENT GAP HEIGHTS BASED ON THE EXPERIMENTAL DATA
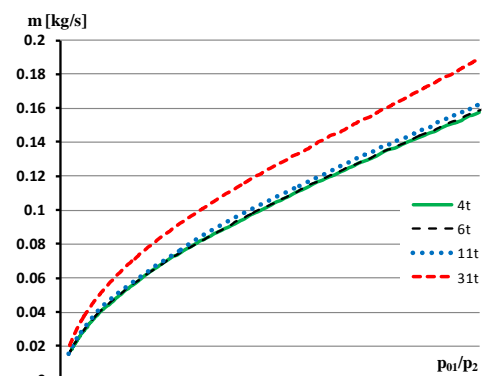
Figure 12 presents the mass flow obtained in the experiment depending on the pressure p_{01}/p_2 ratio for three segments of the geometry LS = 31 mm, B = 1 mm differing by the gap height HG.
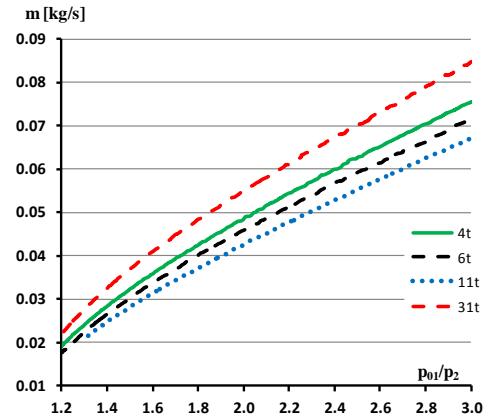
a)
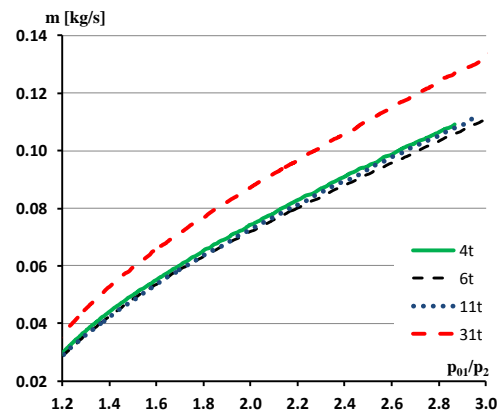
b)

c)

Fig. 12. Mass flow obtained in the experiment depending on the p_{01}/p_2 ratio for the investigated segments of the gap height a) HG = 0.362, b) HG = 0.542, c) HG = 0.752 mm.

From the data related to the segment of the gap height of HG = 0.362 mm (Fig. 12(a)), it results that the number of teeth in the segment is impactful on the leakage. For this gap height, the lowest mass flow was obtained for the segment having 11 teeth in the entire range of the investigated pressure p_{01}/p_2 ratios. For the gap HG = 0.542 mm, the lowest mass flow was obtained for the segments having 6 and 11 teeth (Fig. 10(b)). For the 4-tooth segment, the mass flow is slightly higher. These relations have been presented in detail in Fig. 6. For the segment of the greatest gap height of HG = 0.752 mm, the lowest mass flow was obtained for 4 and 6 teeth. The values of the mass flows for these segment are very similar. A slightly higher mass flow was obtained for the 11-tooth segment. For the analyzed geometries (Fig. 10), the highest mass flow was obtained for the gap seal (31t).

It results from Fig. 12 that the p_{01}/p_2 pressure ratio does not have a significant impact on the range of optimum number of teeth of the investigated segment for each of the analyzed gap heights.

7. CONCLUSION

The geometry of a slot seal is a boundary form of a straight-through labyrinth seal of the maximum leakage value for a given height of the slot of the segment. The results contained in the paper confirm that the change in the leakage level from a straight-through labyrinth seal to a slot seal is smooth.

For a given length of the segment, increasing the number of teeth results in a greater number of places of expansion on one hand and, on the other, in a reduction of the length of the chambers and worse conditions for kinetic energy dissipation. These relations are antagonistic. It is therefore, possible to find such a number of teeth, for which the leakage is minimum.

The mass flow of gas passing through the investigated segments of the seal, obtained in the experiment and in the CFD calculations, indicates a significant influence of the pitch length on the leakage level. A relative change in the mass flow for the analyzed geometries reaches 19% (HG = 0.542 mm).

For the Neumann and Scharrer methods, correction coefficients were proposed for the reference geometry containing 4 teeth. The application of a coefficient in the Neumann method allowed obtaining convergent results for the analyzed segments.

Despite allowing for the thickness of the teeth in the seal, the Scharrer method turned out less accurate than the Neumann method, but it calculated more precisely the number of teeth for the minimum mass flow. Without corrections, the Neumann and Scharerr methods are not overly accurate for the analyzed geometry. The Salzman and Fravi method turned out accurate for the slotted segment.

It results from the measurement data that for the segment of the slot height of 0.542 mm, the range of the number of teeth for the minimum mass flow is

from 6 to 11. The results of the CFD calculations presented in the paper for the segment of the gap height of HG = 0.542 mm allowed a confirmation of the experimentally obtained optimum geometry range. The one-dimensional Neumann and Scharrer methods confirm the occurrence of a minimum mass flow in the experimentally obtained range of the teeth number from 6 to 11.

CFD calculations showed that the lowest mass flow was obtained for the segment containing 9 teeth. This is a result of an optimum relation between the high number of places of expansion and the dissipation of kinetic energy in the chambers, which gives a significant drop of pressure in the segment. A reduction of the pitch length results in a disadvantageous fade of the expansion in the gap caused by high velocity of the gas in the chambers. The dissipation of energy of the gas flow in the chambers is lower if the length of the seal chamber is smaller.

The flow of gas in a straight-through seal of a small pitch (high number of teeth) has a nature of a flow in a labyrinth seal and a slotted seal (great influence of friction on the body walls, the teeth and the shaft). It results from the experimental data for the segments of the gap height of HG = 0.362, 0.542, 0.752 mm that the optimum number of teeth, hence the seal pitch, depend on the gap height. For the investigated segments, the following optimum ranges of the number of teeth were obtained respectively: 11, 6-11, 4-6. We can observe a relation that the smaller the gap the higher the optimum number of teeth. The optimum number of teeth does not depend on the p_{01}/p_2 pressure ratio.

The obtained results indicate a possible direction of improvement of tightness of the straight-through labyrinth seal segments as well as the slotted and groove seals.

REFERENCES

Anker, J., F. Jurgen and H. Stetter (2002). Computational Study of the Flow in an Axial Turbine with Emphasis on the Interaction of Labyrinth Seal Leakage Flow and Main Flow. In E. Krause *et al.* (Ed.), *High Performance Computing in Science and Engineering 2001*, Springer-Verlag Berlin Heidelberg.

Asok, S. P., K. Sankaranarayanasamyb, T. Sundararajanc, K. Rajeshd and G. Sankar Ganeshan (2007). Neural network and CFD-based optimisation of square cavity and curved cavity static labyrinth seals. *Tribology International* 40, 1204–1216.

Childs, D. W. and J. K. Scharrer (1986). An Iwatsubo-Based Solution for Labyrinth Seals: Comparison to Experimental Results. *Journal of Engineering for Gas Turbines and Power* 108 (2), 325-331.

Egli, A. (1935). The leakage of steam through labyrinth seals. *Transactions of the ASME* 57, 115–122.

Frączek, D. and W. Wróblewski (2017). Influence of Honeycomb Rubbing on the Labyrinth Seal Performance. *Journal of Engineering for Gas Turbines and Power* 139 (12502), 1-10.

Hodkinson, B. (1940). Estimation of the Leakage through a Labyrinth Gland. *Proceedings of the Institution of Mechanical Engineers* 141, 283-288.

Joachimiak, D. and P. Krzyślak (2016). A model of gas flow with friction in a slotted seal. *Archives of Thermodynamics* 37 (3), 95-108.

Joachimiak, D. and P. Krzyślak (2017). Investigations into gas flow in a short segment of a straight-through labyrinth seal of high wear level based on experimental research and CFD calculations. *Polish Maritime Research* 2(94) 24, 83-88.

Lampart, P. (2007). Tip leakage flows in turbines. *Task Quarterly* 10 (2), 139-175.

Larjola, J., J. Honkatukia, P. Sallinen and J. Backman (2010). Fluid dynamic modeling of a free piston engine with labyrinth seals. International. *Journal Thermal Science* 19 (2), 141–147.

Martin, H. M. (1908). Labyrinth packings. *Engineering* 85(10), 35-38.

Mel'nik, V. A. (2009). Calculating leaks in rotor-machine radial slot seals. Part 1. Method based on calculated and empirical local pressure loss coefficients. *Chemical and Petroleum Engineering* 45 (9–10), 570-576.

Menter, F. R. (1994). Two-equation eddy-viscosity turbulence models for engineering applications. *American Institute of Aeronautics and Astronautics Journal* 32 (8), 1598-1605.

Nayak, K. C. and P. Dutta (2016). Numerical Investigations for Leakage and Windage Heating in Straight-Through Labyrinth Seals. *Journal of Engineering for Gas Turbines and Power* 138 (12507), 1-10.

Scharrer, J. K. (1988). Theory versus experiment for the rotordynamic coefficients of labyrinth gas seals: Part I – A two control volume model. *Journal of Vibration, Acoustics, Stress and Reliability in Design* 110, 270-280.

Schramm, V., J. Denecke, S. Kim and S. Wittig (2004). Shape Optimization of a Labyrinth Seal Applying the Simulated Annealing Method. *International Journal of Rotating Machinery* 10 (5), 365–371.

Stępień, R. and K. Kosowski (2009). Remarks on aerodynamic forces in seals of turbine stages. *Polish Maritime Research* Special issue S1, 58-63.

Stępień, R., K. Kosowski, M. Piwowarski and J. Badur (2003). Numerical and Experimental Investigations into Pressure Field in Blade Shroud Clearance, Part II: Numerical Analysis. *Task Quarterly* 7 (3), 319-327.

Trutnovsky, K. (1964). *Noncontacting seals; basics and applications of slot and labyrinth fluid-flow seals*, VDI-Verlag bh Dusseldorf, Publishing House of the Association of German Engineers.

Yamada, Y. (1962). On the pressure loss of flow between rotaring co-axial cylinders with rectangular grooves. *Bulletin of the JSME* 5 (20), 642-651.

Yuan, H., S. Pidaparti, M. Wolf, J. Edlebeck and M. Anderson (2015). Numerical modeling of supercritical carbon dioxide flow in see-through labyrinth seals. *Nuclear Engineering and Design* 293, 436-446.

Zhang, W. F., J. G. Yang, C. Li and Y.W. Tian (2014). Comparison of leakage performance and fluid-induced force of turbine tip labyrinth seal and a new kind of radial annular seal. *Computers & Fluids* 105, 125–137.

Zimmerman, H. and K. H. Wolff (1987). Comparison between Empirical and Numerical Labyrinth Flow Correlations. *ASME 87-GT-86*, 35-36.